

Computation of Absolute Hydration and Binding Free Energy with Free Energy Perturbation Distributed Replica-Exchange Molecular Dynamics

Wei Jiang,[†] Milan Hodoscek,[‡] and Benoît Roux^{*,†,§}

Biosciences Division, Argonne National Laboratory,
9700 South Cass Avenue, Building 221 Argonne,
Illinois 60439, Center for Molecular Modeling, National
Institute of Chemistry, Hajdrihova 19, SI-1000 Ljubljana,
Slovenia, and Department of Biochemistry and Molecular
Biology, Gordon Center for Integrative Science, University
of Chicago, 929 57th Street, Chicago, Illinois 60637

Received May 5, 2009

Abstract: Distributed Replica (REPDSTR) is a powerful parallelization technique enabling simulations of a group of replicas in a parallel/parallel fashion, where each replica is distributed to different nodes of a large cluster [*Theor. Chem. Acc.* **2003**, *109*, 140]. Here, we use the framework provided by REPDSTR to combine a staged free energy perturbation protocol with replica-exchange molecular dynamics (FEP/REMD). The structure of REPDSTR, which allows multiple parallel input/output (I/O), facilitates the treatment of replica-exchange to couple the N window simulations corresponding to different values of the thermodynamic coupling parameters. As a result, each of the N synchronous window simulations benefit from the sampling carried out by the N-1 others. As illustrative examples of the FEP/REMD strategy, calculations of the absolute hydration and binding free energy of small molecules were performed using the biomolecular simulation program CHARMM adapted for the IBM Blue Gene/P platform. The computations show that a FEP/REMD strategy significantly improves the sampling and accelerates the convergence of absolute free energy computations.

Introduction

The design of accurate and rapid methods for calculating the free energy of solvation and binding of small molecules is one

of the central goals of computer simulations. Progress in this area could, for example, help speed up the development and prediction of new therapeutic molecules and accelerate drug discovery. In principle, this can be achieved using free energy perturbation (FEP) calculations based on molecular dynamics (MD) simulations of atomic models including explicitly the solvent molecules. To enable robust and effective computations of absolute solvation free energies and of binding free energies, a staged FEP/MD simulation protocol based on a step-by-step decomposition of the total reversible work was developed.^{1–4} The staged protocol effectively breaks down the complete free energy calculation into several independent MD simulations, which are easy to distribute over independent compute nodes. Nevertheless, a treatment based on independent simulations does not exploit all the available information in the computations for the sampling. Furthermore, such a treatment does not make the best possible use of supercomputing platforms allowing massively distributed processes.

One possible strategy to improve the FEP/MD is to couple the staged free energy simulations using replica-exchange methodologies.^{5–12} With REMD, the rate at which the configurations of a system are being explored can be considerably enhanced by attempting coordinate swapping between independent simulations generated at different temperatures^{5,6,11,12} or with different Hamiltonians.^{7–12} Of particular interest, replica-exchange has been combined in Monte Carlo simulations to compute relative free energies.^{7,13} This suggests that REMD might be a promising avenue to further improve FEP/MD simulations. The Distributed Replica (REPDSTR) technique recently developed and implemented in the biomolecular program CHARMM¹⁴ by Hodoscek and co-workers^{15,16} allows multiple MD simulations on similar systems to be simultaneously performed in a highly efficient parallel/parallel mode. In the REPDSTR implementation, each independent MD simulation is treated as an independent replica that occupies a group of processors, and each has its “private” input/output (I/O), including the input script. This is illustrated in Figure 1. REPDSTR is in contrast to the more standard parallel MD, where only the root process deals with the I/O. For this reason, the parallel scaling in REPDSTR is primarily determined by the number of CPUs occupied by each replica, rather than by the total number of CPUs in use. The multiple I/O and parallel structure of REPDSTR greatly facilitate the usage of replica-exchange protocols, with infrequent communication between the separate simulations. It follows that an implementation of a staged FEP protocol with replica-exchange between the different thermodynamic window simulations is relatively transparent and easy to manage. One advantage is that the resulting free energy

* Corresponding author e-mail: roux@uchicago.edu.

[†] Argonne National Laboratory.

[‡] National Institute of Chemistry, Slovenia.

[§] University of Chicago.

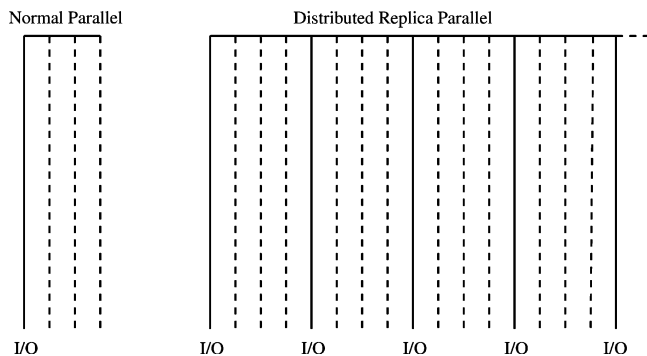


Figure 1. Multiple I/O structure of distributed replica parallel.

perturbation distributed replica-exchange molecular dynamics (FEP/REMD) algorithm is controlled within a single program rather than via an external job-driven script. It is therefore well adapted for massively distributed supercomputing platforms.

In this communication, we describe and implement a computational scheme based on the REPDSTR of CHARMM for computing the absolute hydration and binding free energies within a staged FEP protocol using a replica-exchange MD simulations with λ -swap moves. It is shown that this FEP/REMD scheme improves the sampling efficiency and convergence of free energy computations. FEP/REMD is illustrated with the calculation of the absolute hydration free energy of water and benzene and the absolute binding free energy of camphor-P450 complex.

Computational Details

A. Staged FEP Simulation Protocol. The staged FEP/MD simulation protocol with biasing restraints was described in refs 1–4. Briefly, the insertion of the ligand into the binding pocket is done in three steps, with the help of the three thermodynamic coupling parameters, λ_{rep} , λ_{dis} , and λ_{elec} , controlling the non-bonded interaction of the molecule with its environment. One additional parameter, λ_{rstr} , is used to control the translational and orientational restraints. The potential energy is expressed in terms of the four coupling (window) parameters

$$U(\lambda_{\text{rep}}, \lambda_{\text{dis}}, \lambda_{\text{elec}}, \lambda_{\text{rstr}}) = U_0 + U_{\text{rep}}(\lambda_{\text{rep}}) + \lambda_{\text{dis}} U_{\text{dis}} + \lambda_{\text{elec}} U_{\text{elec}} + \lambda_{\text{rstr}} U_{\text{rstr}} \quad (1)$$

where U_0 is the potential of the system with the noninteracting ligand, U_{rep} and U_{dis} are the shifted Weeks-Chandler-Anderson (WCA) repulsive and dispersive components of the Lennard-Jones potential (introduced in ref 1), U_{elec} is the electrostatic contribution, and u_r denotes the restraining potential that helps improve phase space sampling. The repulsive contribution ΔG_{rep} corresponds to the process

$$U(\lambda_{\text{rep}} = 0, \lambda_{\text{dis}} = 0, \lambda_{\text{elec}} = 0, \lambda_{\text{rstr}} = 1) \rightarrow U(\lambda_{\text{rep}} = 1, \lambda_{\text{dis}} = 0, \lambda_{\text{elec}} = 0, \lambda_{\text{rstr}} = 1) \quad (2)$$

the dispersive contribution ΔG_{dis} corresponds to the process

$$U(\lambda_{\text{rep}} = 1, \lambda_{\text{dis}} = 0, \lambda_{\text{elec}} = 0, \lambda_{\text{rstr}} = 1) \rightarrow U(\lambda_{\text{rep}} = 1, \lambda_{\text{dis}} = 1, \lambda_{\text{elec}} = 0, \lambda_{\text{rstr}} = 1) \quad (3)$$

and the electrostatic contribution ΔG_{elec} corresponds to the process

$$U(\lambda_{\text{rep}} = 1, \lambda_{\text{dis}} = 0, \lambda_{\text{elec}} = 0, \lambda_{\text{rstr}} = 1) \rightarrow U(\lambda_{\text{rep}} = 1, \lambda_{\text{dis}} = 1, \lambda_{\text{elec}} = 1, \lambda_{\text{rstr}} = 1) \quad (4)$$

The free energy ΔG_{rstr} corresponds to the process

$$U(\lambda_{\text{rep}} = 1, \lambda_{\text{dis}} = 1, \lambda_{\text{elec}} = 1, \lambda_{\text{rstr}} = 1) \rightarrow U(\lambda_{\text{rep}} = 1, \lambda_{\text{dis}} = 1, \lambda_{\text{elec}} = 1, \lambda_{\text{rstr}} = 0) \quad (5)$$

The insertion of the ligand or solute into the bulk is calculated according to the same protocol but without the restraint.

B. REPDSTR Implementation. With the REPDSTR module of CHARMM,^{15,16} each λ -staging FEP window is treated as a replica. The hydration free energy calculation is separated into three types of jobs, corresponding to the contributions from the repulsive, dispersive, and electrostatic nonbonded interactions. The binding free energy calculation is separated into four types of jobs, corresponding to the repulsive, dispersive, electrostatic, and restraint contributions. Each replica from the set of replicas within a given type occupies multiple processors, in a parallel/parallel mode. Figure 2 shows the REPDSTR implementation of each interaction type as well as the corresponding coupling parameters and replica labels.

The replica-exchange algorithm follows the conventional Metropolis MC exchange probability with λ -swap moves

$$P(\lambda_{\text{type}}^i \leftrightarrow \lambda_{\text{type}}^j) = \min\{1, e^{-[U(\lambda_{\text{type}}^i, \mathbf{X}^i) + U(\lambda_{\text{type}}^j, \mathbf{X}^j) - U(\lambda_{\text{type}}^j, \mathbf{X}^i) - U(\lambda_{\text{type}}^i, \mathbf{X}^j)]/k_B T}\} \quad (6)$$

where U denotes the total potential energy of the underlying replica, and λ_{type}^i and λ_{type}^j denote the staging parameters. When a move is accepted, then the λ values are exchanged (λ -swap). During the REMD simulation, alternating pairs are considered for exchange attempts. Figure 2 shows these replica pairs for each type of interaction, with even and odd denoting the “alternating” replica exchange mode. This λ -swap replica-exchange protocol could easily be extended to the windows of umbrella sampling simulations.

C. MD Simulation. All the FEP/MD simulations were carried out on the IBM Blue Gene/P cluster Intrepid of Argonne National Laboratory using version c36a1 of the CHARMM program,¹⁴ which was modified for the present study. For the hydration calculations each replica (window) occupies 16 CPUs, while for the binding free energy calculation each replica occupies 64 CPUs. To decrease the computational cost without compromising accuracy, reduced systems of the bulk solution and of the binding site were simulated in which the influence of the surrounding was incorporated by a mean-field treatment. The Spherical Solvent Boundary Potential (SSBP)¹⁷ was used for the bulk simulation, and the Generalized Solvent Boundary Potential (GSBP) was used for the binding site simulations.¹⁸ The hydration FEP calculations were done with 400 explicit water molecules and SSBP at 300 K. The systems were propagated with a 2 fs time step using Langevin dynamics. Calculations based on simulation of 40 and 100 ps with different replica-exchange frequencies were generated and compared. To estimate the statistical convergence of the calculations, 10 independent FEP/REMD simulations runs were performed consecutively starting from the configuration saved at the end of the previous run.

For the binding free energy calculations of the camphor-P450 complex with a fixed number of water molecules, ten 100 ps

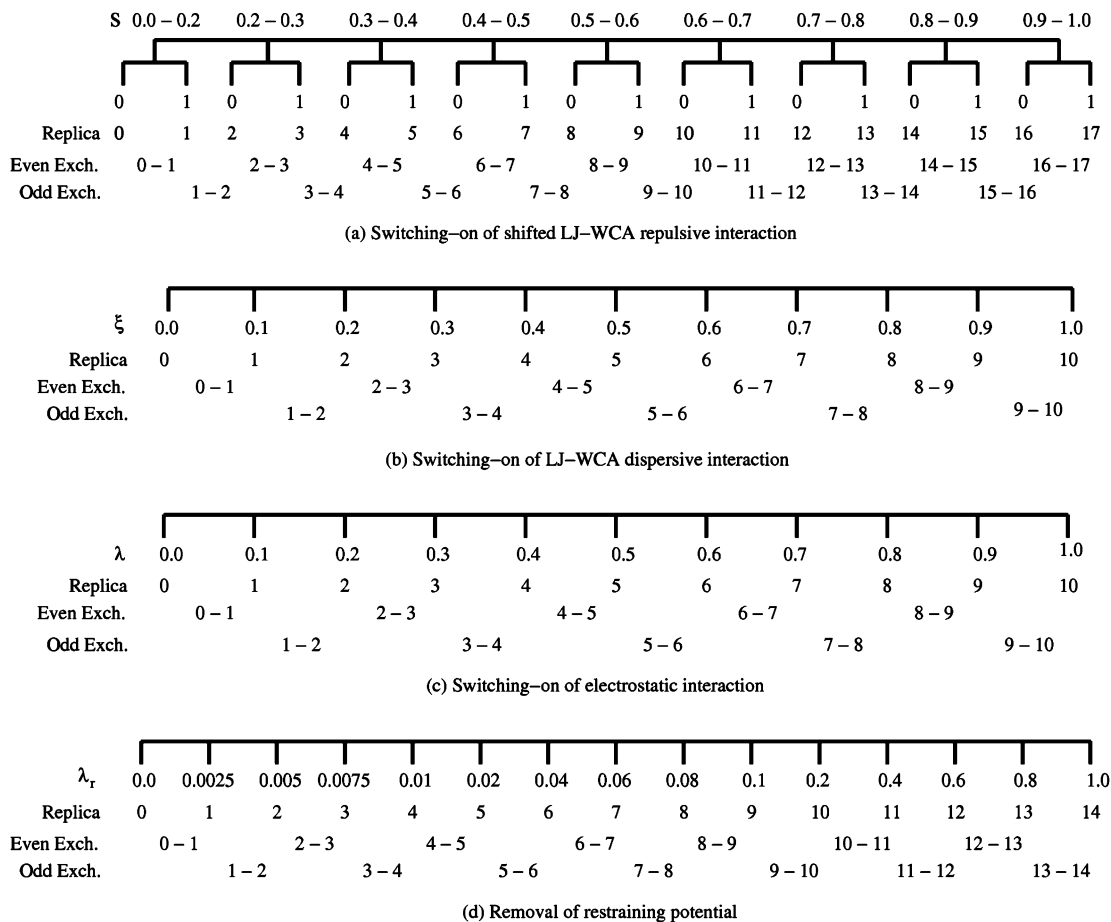


Figure 2. REPDSTR implementation of the staging simulation protocol. Note that the LJ-WCA repulsive interaction is decomposed into 9 stages where each stage consists of two windows with 0 and 1 denoting the initial and final FEP state, respectively. All the windows of the same type were run in a single parallelized job. Each FEP window has its corresponding replica label, and each replica further occupies multiple processors, of which only the root (I/O) process (vertical solid line) is shown. Replica-exchange attempts occur between the two root processes of a selected replica pair.

Table 1. Hydration Free Energy and the Individual Components for Water

MD run	exchange frequency	ΔG_{rep}	ΔG_{disp}	ΔG_{elec}	ΔG	expt
40 ps	0	4.79 ± 0.11	-2.81 ± 0.03	-8.09 ± 0.07	-6.12 ± 0.14	-6.3
	1/1000 steps	5.10 ± 0.16	-2.87 ± 0.01	-8.20 ± 0.12	-5.97 ± 0.23	
	1/100 steps	5.11 ± 0.15	-2.87 ± 0.02	-8.13 ± 0.08	-5.89 ± 0.18	
100 ps	0	5.12 ± 0.10	-2.88 ± 0.01	-8.20 ± 0.05	-5.95 ± 0.11	
	1/1000 steps	5.11 ± 0.06	-2.87 ± 0.01	-8.21 ± 0.07	-5.97 ± 0.12	
	1/100 steps	5.09 ± 0.07	-2.88 ± 0.01	-8.21 ± 0.06	-6.00 ± 0.12	

production runs were performed for the binding site (with GSBP) and hydration, respectively, with a replica-exchange frequency of 1/100 steps. The systems were propagated with a 2 fs time step using Langevin dynamics. The GCMC simulation algorithm, which allows the number of water molecules to fluctuate in equilibrium with an infinite bulk,⁴ was employed with a replica exchange frequency of 1/100 steps. The force field parameters and initial structure of camphor-P450 complex were taken from ref 4. To estimate the statistical convergence of the calculations, 10 independent FEP/REMD simulations (10×100 ps) were performed consecutively for each system with a fixed number of water molecules, each starting from the configuration saved at the end of the previous run. In the FEP simulations combining GCMC and REMD, 30 consecutive calculations were performed to eliminate the influence of structural relaxation on the calculated free energy.

For all calculations, the energies were collected during the production run and postprocessed using the weighted histogram analysis method (WHAM).¹⁹ The results for the hydration free energy of water and benzene in bulk water are given in Tables 1 and 2, respectively. The results for the binding of camphor to cytochrome P450 are summarized in Tables 3 and 4.

Results and Discussions

A. Hydration Free Energy. Tables 1 and 2 report the calculated hydration free energy for water and benzene using different replica-exchange frequencies and simulation length. For each exchange frequency, an acceptance ratio of about 30% to 40% was achieved using the λ -swap moves and the present set of window parameters. A similar acceptance ratio was obtained for the absolute binding free energy calculation. A

Table 2. Hydration Free Energy and Individual Components for Benzene

MD run	exchange frequency	ΔG_{rep}	ΔG_{disp}	ΔG_{elec}	ΔG	expt
40 ps	0	13.46 ± 0.47	-12.63 ± 0.18	-1.88 ± 0.04	-1.05 ± 0.45	-0.87
	1 /1000 steps	14.41 ± 0.31	-13.07 ± 0.06	-1.89 ± 0.06	-0.55 ± 0.29	
	1/100 steps	14.45 ± 0.39	-13.01 ± 0.07	-1.85 ± 0.05	-0.41 ± 0.39	
	1/10 steps	14.67 ± 0.45	-13.07 ± 0.07	-1.90 ± 0.10	-0.30 ± 0.50	
100 ps	0	14.47 ± 0.20	-13.06 ± 0.06	-1.87 ± 0.04	-0.45 ± 0.19	
	1/1000 steps	14.50 ± 0.21	-13.06 ± 0.04	-1.86 ± 0.06	-0.42 ± 0.18	
	1/100 steps	14.49 ± 0.11	-13.03 ± 0.05	-1.86 ± 0.03	-0.41 ± 0.13	
	1/10 steps	14.49 ± 0.13	-13.03 ± 0.08	-1.86 ± 0.07	-0.41 ± 0.15	

Table 3. Binding Site Free Energies of Camphor-P450 Complex with a Fixed Number of Water Molecules at Binding Site and Hydration Free Energies of Camphor

	binding site		bulk water		expt
	fixed number of water (MD)	fixed number of water (REMD)	MD	REMD	
ΔG_{rep}	7.99 ± 0.13	8.32 ± 0.29	21.15 ± 0.21	21.06 ± 0.30	..
ΔG_{disp}	-35.50 ± 0.06	-35.97 ± 0.03	-21.15 ± 0.15	-21.12 ± 0.08	..
ΔG_{elec}	-1.52 ± 0.04	-1.25 ± 0.04	-4.80 ± 0.04	-4.82 ± 0.04	..
$\Delta \Delta G_{\text{rstr}}$	9.98 ± 0.03	10.07 ± 0.04
sum	-19.05 ± 0.14	-18.83 ± 0.33	-4.80 ± 0.15	-4.88 ± 0.30	-3.5
ΔG_{b}^0	-14.25 ± 0.21	-13.95 ± 0.55	-7.75

Table 4. Binding Free Energies of Camphor to p450

	MD run	ΔG_{rep}	ΔG_{disp}	ΔG_{elec}	ΔG_{b}^0	expt
GCMC-REMD	run 0–9	13.63 ± 1.23	-36.10 ± 0.10	-1.21 ± 0.02	-8.73 ± 1.43	-7.75
	run 10–19	15.61 ± 0.83	-36.18 ± 0.03	-1.24 ± 0.02	-6.86 ± 0.99	
	run 20–29	15.76 ± 0.56	-36.19 ± 0.03	-1.24 ± 0.02	-6.71 ± 0.69	
GCMC-MD	run 0–9	13.58 ± 1.19	-36.00 ± 0.03	-1.30 ± 0.01	-8.87 ± 1.31	
	run 10–19	14.32 ± 0.53	-36.05 ± 0.02	-1.29 ± 0.03	-8.16 ± 0.48	
	run 20–29	15.75 ± 0.73	-36.20 ± 0.05	-1.31 ± 0.03	-6.91 ± 0.64	

higher acceptance ratio can be obtained by increasing the number of windows but that would also increase the computational cost. The statistical uncertainties (standard deviation) for the total hydration free energy and the various components were calculated from the 10 separate production runs.

For the solute water molecule, the total hydration free energy from the 100 ps production runs converges toward a value of -6.0 kcal/mol. The three individual contributions are more informative of the performance of the FEP/REMD than the total free energy, as they display different convergences. The electrostatic and dispersive components converge, consistent with the observation that switching those relatively “soft” interactions is not associated with any sudden reorganization of the surrounding bulk. In contrast, the convergence of the repulsive component is more clearly improved by replica-exchange. The trends are clearer with the 40 ps production runs. With straight FEP/MD (no replica-exchange), the value of ΔG_{rep} is 4.97 kcal/mol (based on 10 independent runs), which systematically deviates by ~ 0.3 kcal/mol from the converged value of 5.09 kcal/mol. Such deviation disappears when replica-exchange is attempted every 1000 or 100 steps. This observation is consistent with the fact that extensive sampling is necessary to sample the cavity formation associated with the repulsive solute–solvent interaction. With FEP/REMD, the ΔG_{elec} calculated from the 100 ps runs is essentially unchanged compared to the 40 ps runs, though the uncertainty is slightly smaller. The two nonpolar components converge well; the averaged ΔG_{rep} and ΔG_{disp} of the 40 ps FEP/REMD runs are almost the same as those of 100 ps runs, regardless of the relatively larger uncertainty due to shorter sampling.

Benzene provides a more interesting testing ground to illustrate the gain by FEP/REMD because of its larger size. The absolute hydration free energy of benzene calculated from 10 independent 40 ps production runs without replica-exchange (-1.05 kcal/mol) deviates systematically from the best-converged value obtained by FEP/REMD (-0.41 kcal/mol). This demonstrates the enhanced convergence from FEP/REMD. With respect to the impact of increasing the replica-exchange frequency and the sampling time, the individual components display similar trends as water shown in Table 1. In the 40 ps runs, the largest deviation again comes from ΔG_{rep} and a systematic deviation of almost -1.0 kcal/mol is avoided by replica-exchange. It is also noteworthy that the contribution from van der Waals dispersion (-12.63 kcal/mol) deviates systematically from the converged value (-13.03 kcal/mol).

The statistical uncertainty in the 40 ps simulation runs exhibits a curious “turnover” with increasing exchange frequency, i.e., the statistical uncertainty is larger when replica exchanges are attempted every 10 steps (± 0.45 kcal/mol) than every 1000 steps (± 0.31 kcal/mol). It is likely that the cause of this is the difficulty to sample the cavity formation associated with the harsh solute–solvent repulsive interaction. With higher exchange frequency, the trajectories jump along the λ_{rep} coupling parameter rapidly, which results in larger fluctuations in the energy samples. This situation is hidden for small solutes such as a water molecule, while the larger benzene molecule requires a more important surrounding reorganization of the solvent upon solute insertion. These observations suggest that a systematic investigation of the relation between the exchange frequency and length of MD trajectory should be the object of further

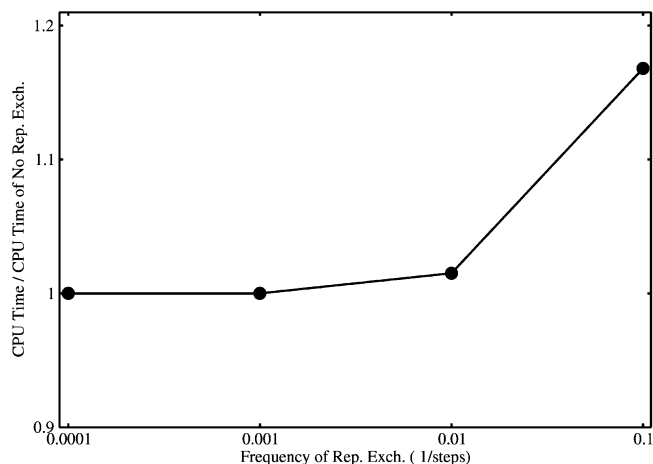


Figure 3. Cost of replica-exchange MD simulation relative to that without replica-exchange. The CPU time of simulation without replica-exchange is denoted with exchange frequency 1/10000 steps (0.0001).

analysis. Of relevance to such issues, it was recently shown that Hamiltonian replica exchange provides a direct route for minimizing the hysteresis error in hydration free energy calculations.²⁰

As shown in Tables 1 and 2, the free energy with replica-exchange converges better with increased exchange frequency. To assess the additional computational cost associated with the exchanges, Figure 3 shows the CPU time of FEP/REMD relative to that of FEP simulations without replica-exchange. It can be seen that with exchange frequencies up to 1/100 steps, there is no significant increase of the CPU time, while for 1/10 steps, the CPU time increases by $\sim 17\%$. Thus, an exchange frequency of $\sim 1/100$ steps seems to be an optimal choice with the current FEP/REMD implementation.

B. Binding Free Energy. The convergence of a calculation of the absolute binding free energy of camphor for p450 is challenging because the binding site is deeply buried within the protein and is not solvent accessible. For this reason, the movement of water molecules in and out of the binding pocket is extremely slowly. This is expected to complicate the convergence of FEP/MD calculations. It was shown previously that the contribution from the repulsive interaction is grossly underestimated in FEP/MD calculations initiated from the structure of the bound complex with a fixed number of water molecules in the buried site. Reasonable results are obtained if the number of water molecules is allowed to fluctuate via a GCMC algorithm.⁴ It is of interest to test if replica-exchange without GCMC is able to cure this problem. To this end, the FEP/REMD calculation was first performed with a fixed number of water molecules corresponding to the X-ray structure of the bound camphor-P450 complex. In Table 3, it can be seen that REMD does not actually improve the convergence of the repulsive interaction contribution. The resulting binding free energy is too favorable by almost 5–6 kcal/mol, similar to previous results.⁴ This shows that the FEP/REMD scheme, by itself, is unable to enhance the sampling of different number of water molecules in the buried binding pocket. Combining replica-exchange with GCMC and MD to perform FEP calculations appears to be necessary in this case. Table 4 gives the results for the calculations performed within a FEP/GCMC-

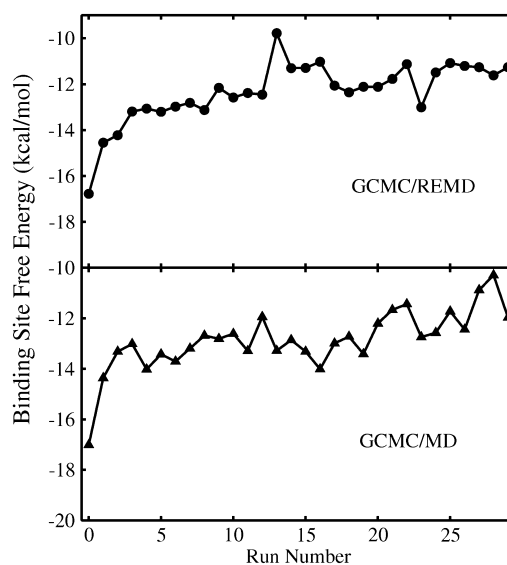


Figure 4. Binding site free energy convergence of GCMC/(RE)MD simulations. Note that GCMC/REMD shows faster convergence than GCMC/MD simulation.

REMD scheme and compares those with the FEP/GCMC-MD. It can be seen that both methods yield a reasonable total binding free energy, indicating that the GCMC algorithm is essential to treat the buried p450 binding site. Again, the repulsive free energies estimated from FEP/GCMC-REMD converged better than that from FEP/GCMC-MD simulation. For the absolute hydration free energy of camphor in bulk water, no noticeable gain is observed with FEP/REMD compared to FEP/MD. In both approaches, the repulsive and dispersive interactions nearly cancel out. This is consistent with the previous results with water and benzene (Tables 1 and 2).

Table 4 shows that from the 10th MD run the repulsive free energies are essentially converged to 15.6 kcal/mol, whereas the corresponding results from the FEP/GCMC-MD simulation are underestimated by ~ 1.4 kcal/mol. Ultimately, the average repulsive free energies of both methods reach a value about 15.75 kcal/mol but only after the 20th run. Figure 4 provides a more detailed picture for the convergence of FEP/GCMC-REMD calculations. One can see that some structural relaxation dominates the early stage of the simulations with and without replica-exchange. The free energy from the FEP/GCMC-REMD simulations starts to fluctuate around a stable value of -12.0 kcal/mol from the 12th run. In contrast, the FEP/GCMC-MD calculation seems to be drifting up even after the 20th run. This shows that replica-exchange significantly accelerates the configurational sampling of the receptor–ligand–solvent complex. The calculation of the electrostatic and dispersive contributions benefits less markedly from REMD, probably because they are switched-on after the formation of a cavity and the fluctuations of the surrounding water molecules are smaller. As observed in Table 4, the dispersion free energy and charging free energy of FEP/GCMC-REMD are very close to the results from FEP/GCMC-MD. The introduction of replica-exchange does not have a large impact in the case of the geometrical restraining potential (Table 3).

Conclusion

A free energy perturbation staging protocol with replica-exchange molecular dynamics (FEP/REMD) implemented

with a distributed in a parallel/parallel mode replica strategy REPDSTR has been described and implemented for large supercomputing platforms. As a natural outcome of this implementation, replica-exchange over configuration with different thermodynamic coupling parameters was shown to enhance the sampling for the calculation of hydration free energies. The benefit is most striking in the case of the repulsive contribution to the free energy (related to the cavity formation). This would be expected to hold in general for ligand binding at the solvent-exposed site near the surface of a receptor. For the deeply buried binding site, the REMD combined with the GCMC algorithm significantly accelerates the free energy convergence. Applications to the present FEP/REMD method to produce a general protocol to different ligand binding processes are currently underway.

Acknowledgment. We would like to acknowledge Dr. Ray Loy for his help with CHARMM on the Blue Gene/P Intrepid of Argonne National Laboratory, Dr. Paul Maragakis for the collaboration building replica-exchange in the REPDSTR module, and Dr. Yuqing Deng, Dr. Sanghyun Park, and Dr. Albert Lau for valuable discussions about free energy calculations and replica-exchange scheme. This research is funded by grant MCB-0920261 from the National Science Foundation. This research used resources of the Argonne Leadership Computing Facility at Argonne National Laboratory, which is supported by the Office of Science of the U.S. Department of Energy under contract DE-AC02-06CH11357.

References

- (1) Deng, Y.; Roux, B. *J. Phys. Chem.* **2004**, *108*, 16567–16576.
- (2) Deng, Y.; Roux, B. *J. Chem. Theory Comput.* **2006**, *2*, 1255–1273.
- (3) Wang, J.; Deng, Y.; Roux, B. *Biophys. J.* **2006**, *91*, 2798–2814.
- (4) Deng, Y.; Roux, B. *J. Chem. Phys.* **2008**, *128*, 115103.
- (5) Rick, S. W. *J. Chem. Theory Comput.* **2006**, *2*, 939–946.
- (6) Rhee, Y. M.; Pande, V. S. *Biophys. J.* **2003**, *84*, 775–786.
- (7) Woods, C. J.; Essex, J. W.; King, M. A. *J. Phys. Chem.* **2003**, *107*, 13703–13710.
- (8) Fajer, M.; Hamelberg, D.; McCammon, J. A. *J. Chem. Theory Comput.* **2008**, *4*, 1565–1569.
- (9) Min, D.; , H.; , L.; , G.; , L.; , R.; , B.- P.; , W., Y. *J. Chem. Phys.* **2007**, *126*, 144109.
- (10) Sugita, Y.; Okamoto, Y. *Chem. Phys. Lett.* **1999**, *314*, 141–151.
- (11) Sugita, Y.; Kitao, A.; Okamoto, Y. *J. Chem. Phys.* **2000**, *113*, 6042–6051.
- (12) Mitsutake, A.; Okamoto, Y. *Phys. Rev. E* **2009**, *79*, 047701.
- (13) Woods, C. J.; Essex, J. W.; King, M. A. *J. Phys. Chem. B* **2003**, *107*, 13711–13718.
- (14) Brooks, B. R.; et al. *J. Comp. Chem.* **2009**, *30*, 1545.
- (15) Woodcock, H. L., III.; Hodoseck, M.; Gilbert, A. T. B.; Gill, P. M. W.; Schaefer, H. F., III.; , R., B. B. *J. Comput. Chem.* **2007**, *28*, 1485–1502.
- (16) Woodcock, H. L., III.; Hodoseck, M.; Sherwood, P.; Lee, Y.; Schaefer, H.; Brooks, B. *Theor. Chem. Acc.* **2003**, *109*, 140–148.
- (17) Beglov, D.; Roux, B. *J. Chem. Phys.* **1994**, *100*, 9050–9063.
- (18) Im, W.; Berneche, S.; Roux, B. *J. Chem. Phys.* **2000**, *114*, 2924–2937.
- (19) Kumar, S.; Bouzida, D.; Swendsen, R. H.; Kollman, P. A.; Rosenberg, J. M. *J. Comput. Chem.* **1992**, *13*, 1011–1021.
- (20) Wyczalkowski, M. A.; Pappu, R. V. *Physical Review* **2008**, *77*, 026104.

CT900223Z